Materials Science-Poland, 31(4), 2013, pp. 506-515
http://www.materialsscience.pwr.wroc.pl/
DOI: 10.2478/s13536-013-0133-5

VERSITA

Identification of growth mechanism of CBD CIAS thin films from SEM analysis

B. KAVITHA*, M. DHANAM

Department of Physics, Kongunadu Arts and Science College, Coimbatore-641029.

Near stoichiometric and stoichiometric $CuIn_{(1-x)}Al_{(x)}Se_2$ (CIAS) thin films have been prepared by chemical bath deposition (CBD) technique. X-ray diffraction (XRD) and energy dispersive x-ray analysis (EDAX) spectra have been employed to confirm the structure and composition of the prepared films. SEM analysis of near-stoichiometric and stoichiometric CIAS thin films enabled us to estimate the grain size, to identify the growth mechanism and also to visualize the surface morphology. Transmittance spectra have been employed to determine the type of transition and other optical parameters such as absorption coefficient, extinction coefficient, dielectric constant, refractive index, Sellmeier parameters and bandgap which are reported in this paper in detail.

Keywords: *CBD; SEM; XRD; EDAX; stoichiometric and near-stoichiometric CIAS thin films*

1. Introduction

Thin film solar cells based on chalcopyrite thin films have gained increasing interest due to steady progress in conversion efficiencies [1]. Solar cells based on chalcopyrite compound $CuInSe_2$ [CIS] thin films emerged as a leading absorber candidate for low cost solar electric power generation twenty years ago [1]. Several recent advances have been made to improve its band gap (Eg). The band gap of CIS can be increased to match the solar spectrum for higher efficiency by alloying with group III or IV elements. Extensive research work has been carried out on $Cu(In,Ga)Se_2$ (CIGS) and $CuIn(S,Se)_2$ (CISS) alloy systems. Significant effort has been made to develop high-efficiency solar cells with an increased band gap by gallium additions i.e. $CuIn_{1-x}Ga_xSe_2$ films and devices. Currently the highest conversion efficiency reported is 20.3 % for $Cu(In,Ga)Se_2$ (CIGS) solar cells [2]. The band gap of CIGS can be varied from 1.0 to 1.7 eV. However, with band gaps greater than 1.3 eV, the efficiency of CIGS devices is limited by a degradation of the electronic properties of the CIGS layer leading to losses in the fill factor (FF) and open circuit voltage (Voc) and a decrease in the junction quality factor [3, 4]. $Cu(InAl)Se_2$ (CIAS) may be a viable alternative for higher band gap CIS-based solar cells because it requires a smaller relative alloy concentration than Ga or S alloys to achieve a comparable band gap. Thus $CuIn_{(1-x)}Al_{(x)}Se_2$ (CIAS) is a viable alternative for higher bandgap absorbers and is attractive to thin film solar cell production. The highest confirmed 16.9 % conversion efficiency has been reported for CIAS solar cells [5].

CIAS thin films have been prepared by several techniques including co-evaporation [6–10] and sequential deposition methods [11–13]. In the present work CIAS thin films have been grown by chemical bath deposition (CBD) technique in which the deposition occurs when the substrate is maintained in contact with dilute chemical bath containing reaction mixture. The film formation on the substrate takes place when the amount of ionic product (IP) exceeds the amount of solubility product (SP). Among various CBD techniques, a non-vacuum electroless technique has many advantages such as simplicity, no requirement for sophisticated instruments, minimum material wastes, economical way of large area deposition, no need of handling poi-

*E-mail: kavitha_48@yahoo.co.in

sonous gases like H_2Se or Se vapour and possibility of room temperature deposition. In view of these advantages, CBD technique has been selected for the preparation of CIAS thin films. Moreover, the literature survey revealed that no researchers have performed the surface morphological analysis of CBD CIAS thin films in detail. Hence, it has been planned to carry out a systematic study on the structure, surface morphology and optical properties of near-stoichiometric and stoichiometric CBD CIAS thin films.

2. Experimental details

Near-stoichiometric and stoichiometric CBD CIAS thin films were prepared from the reaction mixture containing copper sulphate (⩾99 % purity – Merck), trisodium citrate (⩾99 % purity – Merck), indium trichloride (⩾99.999 % Sigma Aldrich), selenium (⩾99.99 % Sigma Aldrich) aluminium sulphate (⩾99 % purity – Nice) and citric acid (⩾99 % purity – Merck). All solutions were prepared in double distilled water and the chemicals used with different concentration and volume for near stoichiometric and stoichiometric CIAS thin films are presented in Table 1. A digital pH meter (model 101 E-Electronic India) has been used to adjust the pH of the reaction mixture. The pH meter was standardized using buffer solutions of pH 4 ± 0.05 and 9.2 ± 0.05. The substrates used for the deposition of the films were suspended closer to the inner wall of the deposition beaker for better uniformity and adherence of the film onto the substrates and to avoid shaking of the substrates while deposition [14]. A constant and very slow stirring was provided while adding the different solutions to the reacting mixture. $CuSO_4$ solution was taken in a 100 ml beaker, TSC solution was then added drop by drop to it followed by sodium selenosulfite (Solution A). Citric acid was used as a complexing agent for $InCl_3$ and Al_2SO_4 and this solution was added drop by drop to solution A (reaction mixture). The pH of the reaction mixture was varied from 9 to 10 and optimized as 10 [15] and the deposition time was optimized in the range of 30 to 120 minutes to obtain films of uniform thickness. The depositions were carried out in water bath at two different temperatures (50 °C and 60 °C) and optimized as 60 °C. When the concentration of copper sulphate was varied from 0.5 M to 0.2 M, Cu-rich and Cu-poor CIAS thin films, were obtained. The concentration of indium trichloride and aluminium were changed to obtain In-rich and In-poor thin films without changing the volume of the solution (Table 1). The preparation conditions of stoichiometric CIAS thin films have also been presented in Table 2. After deposition the films were taken out and dried naturally.

2.1. Characterization

The thickness of the prepared CIAS films was determined by a gravimetric technique and the films were annealed at 100 °C for one hour and used for the analysis. Structural characterization of these films was carried out by using Shimadzhu (Lab X-6000) X-ray diffractometer with Cu K_a ($\lambda = 1.5406$ Å) line in 2θ range from 20 to 80 degrees. Compositional and morphological characterization of these films was carried out by using Hitachi Model: S-3400N.

3. Results and discussion

3.1. EDX analysis

Fig. 1(a) shows the representative EDX spectrum of a 625 nm thick CBD CIAS thin film revealing the presence of the chemical constituents: Cu, In, Al and Se. EDX quantitative results confirm the atomic percentage of the constituents in the prepared films as well as the composition of near stoichiometric and stoichiometric CBD CIAS thin films (Table 3).

3.2. XRD analysis

A representative x-ray diffraction pattern of CBD CIAS stoichiometric thin film of 625 nm thickness is presented in Fig. 1(b). The prepared films were found to be polycrystalline in nature and exhibiting chalcopyrite structure. From the diffraction profiles the diffraction angles and the intensity of lines were measured with high accuracy. Possible directions in which the films diffracted the beam of monochromatic x-rays were

Table 1. Concentration and volume of the chemicals used for the preparation of near-stoichiometric CBD CIAS thin films.

Chemicals	Concentration (M)				Volume (ml)			
	Cu-rich	Cu-poor	In-rich	In-poor	Cu-rich	Cu-poor	In-rich	In-poor
Copper sulphate	***0.5***	***0.2***	0.2	0.2	15	15	7.5	7.5
Trisodium citrate	0.1	0.1	0.1	0.1	10	10	7.5	7.5
Citric acid	0.1	0.1	0.1	0.1	20	20	25	25
Indium trichloride	0.1	0.1	***0.2***	***0.1***	10	10	12.5	12.5
Aluminium sulphate	0.1	0.1	***0.1***	***0.125***	10	10	12.5	12.5
Sodiumselenosulphite	0.1	0.1	0.1	0.1	20	20	40	40

Table 2. Concentration and volume of the chemicals used for the preparation of stoichiometric CBD CIAS thin films.

Chemicals	Concentration (M)	Volume (ml)
Copper sulphate	0.2	20
Trisodium citrate	0.1	10
Citric acid	0.1	20
Indium trichloride	0.2	10
Aluminium sulphate	0.15	10
Sodiumselenosulphite	0.1	40

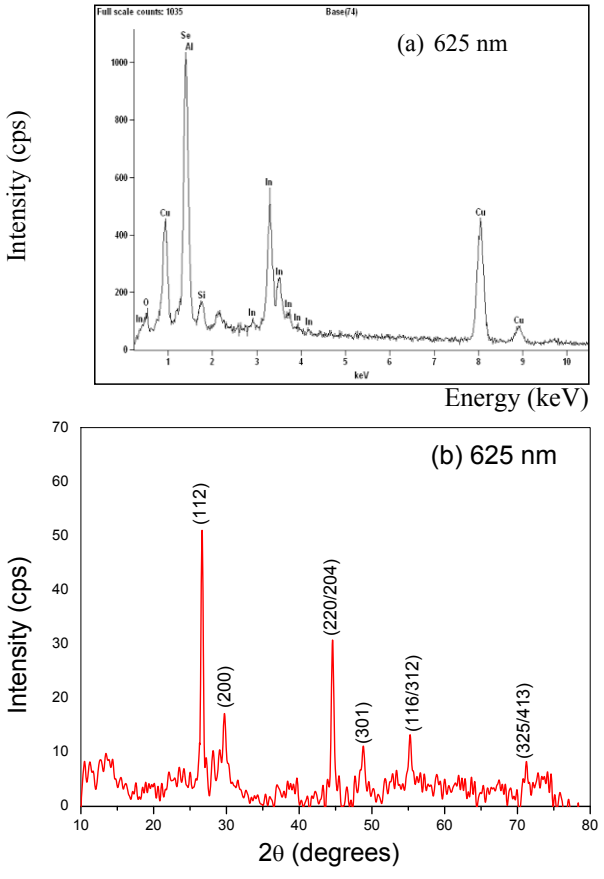

Fig. 1. (a) EDAX (b) XRD spectra of a representative CBD CIAS thin films.

determined by Bragg's equation [16]. The crystallites were found to have main peak orientations along (112), (200), (204/220) (116/312), (301) and (325/413) directions. The absence of CuSe crystals was also confirmed by the absence of CuSe peaks ((111) or (444)) in the XRD spectra (Fig. 1(b)). Since no Joint Committee on Powder Diffraction Standards (JCPDS) file was available for CIAS, $CuInSe_2$ (JCPDS No.40-1487) and $CuAlSe_2$ (JCPDS No.44-1269) standards were used and the results were compared with earlier reports [6–13]. The extra-protruding background in the 2θ range originates from the diffraction of glass substrates [17]. The estimated lattice constants, tetragonal structure and various structural parameters have been reported elsewhere [15].

3.3. Morphological analysis

CBD CIAS thin films contain different types of grains due to the variation in Cu/(In+Al) ratio. Merdes [18] reported that the significant difference in homogeneity and grain size observed might be the indication of the strong dependence between precursor composition and absorber structural properties. SEM micrographs (Fig. 2) illus-

Table 3. EDX quantitative results of CBD CIAS thin films.

Near-stoichiometric CBD CIAS Films	Atomic percentage (%)				Film composition
	Cu	In	Al	Se	
Slightly Cu-rich (t = 800 nm)	27	11.32	11.20	50.49	$Cu_{1.1}(In_{0.45}Al_{0.55})Se_2$
Slightly Cu-poor (t = 750 nm)	23	13.19	12.11	51.36	$Cu_{0.92}(In_{0.52}Al_{0.48})Se_2$
Slightly In-rich/Al-poor (t = 450 nm)	23.64	14.41	11.10	50. 94	$Cu_1(In_{0.57}Al_{0.44})Se_2$
Slightly In-poor/Al-rich (t = 600 nm)	25.17	10.48	12.87	50.54	$Cu_1(In_{0.42}Al_{0.51})Se_2$

Stoichiometric CBD CIAS films	Cu	In	Al	Se	Film composition
(t = 500 nm)	25.02	12.50	12.51	50.8	$CuIn_{0.5}Al_{0.5}Se_2$
(t = 625 nm)	25.13	12.49	12.51	51.0	$CuIn_{0.49}Al_{0.50}Se_2$
(t = 710 nm)	25.40	12.51	12.48	50.7	$CuIn_{0.5}Al_{0.49}Se_2$

trate the dependence of film surface morphology on the film composition. It can be observed that slightly Cu-rich CIAS films have a rough surface morphology with a certain degree of non-uniformity in the grain size [19, 20]. The picture shows the co-existence of small and relatively large grains with an average grain size of 2 μm on the film surface [12]. Similar observations were made in CIS material composed of two types of grains (bigger and smaller) where the bigger grain growth was more appropriate to produce photovoltaic cells with high efficiency [21] whereas the small-grained absorber layers were useful for highly efficient solar cells [2]. The surface morphology implies that the growth of a slightly Cu-rich film is near isotropic. The growth under slightly Cu-rich conditions leads to the presence of the chalcogenide phase with large grain size as suggested by Zoppi et al. [22]. This was confirmed in the present study by the higher grain size of slightly Cu-rich CIAS thin films (2 μm) compared with slightly Cu-poor CIAS thin films (0.5 μm). The slightly Cu-poor CIAS films were strongly faceted and contained small particles with the size of ∼0.5 μm. The observed rose-like morphology of CIAS thin films was confirmed as the morphology of Cu-deficient CIS thin film by L.C. Yang et al. [23]. Slightly Cu-rich CIAS thin film is dense whereas slightly Cu-poor CIAS thin film contains significantly more voids. The morphology of slightly Cu-poor CBD CIAS thin film is completely dominated by multinuclear, spherical, outward growth, which typically leads to the formation of large size clusters. Due to such morphology, a very large surface area is required for CIAS thin films. This is a positive quality as far as large area CIAS thin films with minimum rugosity factor are concerned, as reported elsewhere [24] for CBD CIS thin films.

The morphology of In-rich films is totally different from that of slightly Cu-rich film. The grain size of slightly In-rich CIAS thin film is smaller compared with the slightly Cu-rich one (Table 4). This may be explained by the mobility of Cu^+ ions [25, 26]. The platelet like slightly In-rich film structure may be derived from a twin-plane re-entrant edge growth mechanism as suggested by Artaud et al. [27]. Fig. 2 (SEM of slightly In-rich CIAS thin films) corresponds to the backscattering topography where the chemical contrast is evidenced. The presence of In makes the grain appear white, whereas the grey ones only contain Cu, Al and Se. Moreover, an increase of In content leads to the decrease of the grain size because the grain begins to appear on the top of the surface which is also related to the diminution of the growth rate [27]. A non-compact sur-

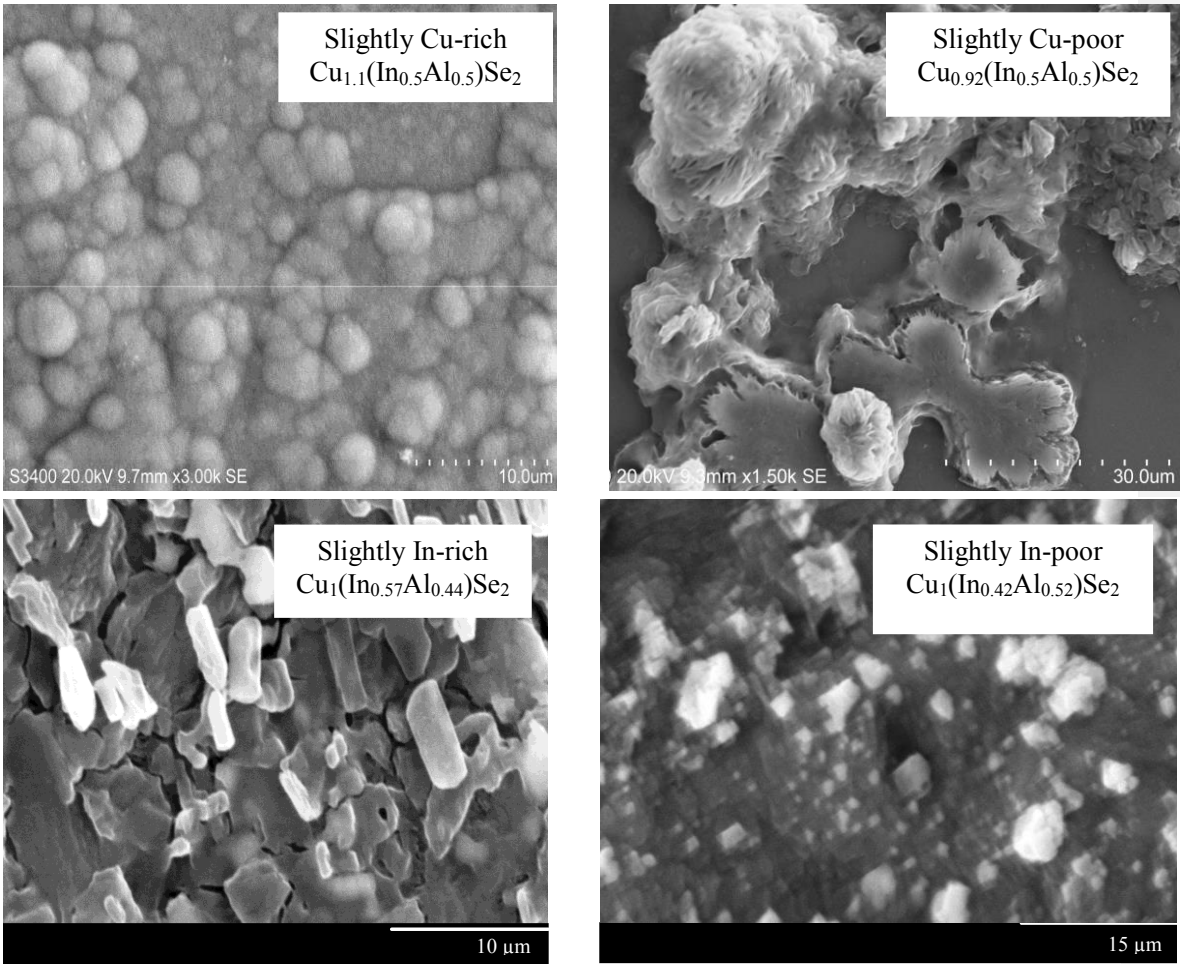

Fig. 2. SEM micrographs of near-stoichiometric CBD CIAS thin films.

face composed of separated grains, clusters and agglomerates was observed in slightly In-rich CIAS thin films earlier [27]. When atomic percentage of indium decreases, a very compact structure composed of spherically shaped grains with typical size varying approximately between 1.5 and 2 µm is observed [28–31]. When In content decreases, the grain size is found to increase in slightly In-poor CIAS thin film as suggested earlier [28]. Voids are present in slightly In-poor films and the film morphology suggests that the growth is near isotropic.

Scanning electron micrographs of stoichiometric CBD CIAS thin films (Fig. 3) show irregular islands and cube shaped grains. All the samples showed a good adhesion to the glass substrates. Olenjeck [32] reported that CIAS thin films had some unwanted phases and impurities such as $Cu_{2-x}Se$ and pure unreacted Se. The absence of hexagonal plates in the micrographs suggested the absence of CuSe crystals which was also confirmed by the absence of CuSe peaks ((111) or (444)) [27] in the XRD spectra (Fig. 1(b)). The absence of white rods suggested the absence of unreacted Se or the complete formation of CIAS. The absence of white patches (indium segregation) enhanced the morphology of the absorber film and the film had uniform grey appearance [33]. The morphological study of CBD CIAS thin films suggested that stoichiometric films had relatively larger grains than near-stoichiometric CBD CIAS thin films. Hayashi et al. [34] reported that the surface roughness (rms roughness) of CIAS thin film was influenced by Cu/In (Cu/III_{nd}) ratio. They found that the surface roughness increased for Cu/III_{nd} ratio up to 1.3 and

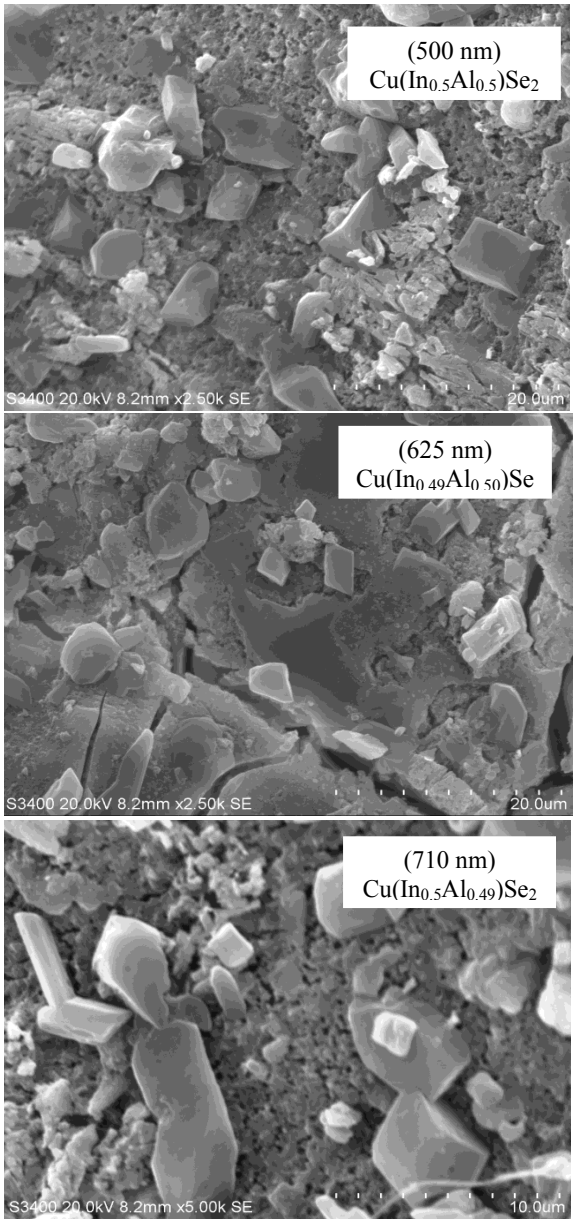

Fig. 3. SEM micrographs of stoichiometric CBD CIAS thin films.

saturated for the ratio values greater than 1.3. The prepared near-stoichiometric as well as stoichiometric CBD CIAS thin films have Cu/III$_{nd}$ ratio $>$1.6 (Table 4) and therefore they have the saturated roughness.

The grain sizes of CBD CIAS thin films (Table 4) are larger than the film thickness (Table 3) and therefore the grains extend unbroken in the surface. This is a positive attribute of this semiconducting material as the large grains minimize the grain boundaries and reduce the detrimental effect on conductivity and carrier recombination. Furthermore, the minority carriers can pass through the film without crossing the grain boundary as reported earlier [22]. The large grain size and the columnar-shaped crystals are advantageous to the collection of photo-generated carriers [34]. The results of SEM analysis of CBD CIAS thin films are presented in Table 4 and enable us to conclude that both near-stoichiometric and stoichiometric CBD CIAS thin films are suitable for solar cell applications.

3.4. Optical analysis

Fig. 4 shows the transmittance spectra of near stoichiometric and stoichiometric CIAS thin films. It can be observed that in both near stoichiometric and stoichiometric thin films the absorbance increases with the increase in film thickness as observed by earlier studies for CIS and CIAS thin films [6, 24]. A representative plot of $(\alpha h\upsilon)^2$ versus $h\nu$ for near stoichiometric and stoichiometric CIAS thin films is presented in Fig. 5. The plot confirms that the prepared films have direct allowed transitions and the average band gap energies estimated from the plot are in the range of 1.27 – 1.42 eV and 1.24 – 1.44 eV, respectively (see Table 5). But the increase in band gap values from 1 eV (CIS) to 1.2 – 1.5 eV (CIAS) confirms the replacement of indium atoms by aluminium. The observed band gap energies are in a very good agreement with reported values for CIAS thin films [3, 6, 8–10, 12, 13, 38, 39] and they decrease with the increase in film thickness. This may be due to the increase in crystallite size and a decrease in strain leading to a decrease in band gap energy [40]. The plots $(\alpha h\upsilon)^{1/2}, (\alpha h\upsilon)^{1/3}, (\alpha h\upsilon)^{3/2}$ versus photon energy ($h\nu$) were plotted for both near-stoichiometric and stoichiometric CIAS thin films, revealing that the CIAS thin films did not have direct forbidden and indirect transitions.

3.5. Estimation of optical parameters

The optical parameters such as absorption coefficient (α), extinction coefficient (k), refractive in-

Table 4. Results of SEM images of CBD CIAS thin films.

Film composition	(Cu/In) ratio	Grain size (μm)	Film Morphology	Growth Mechanism	Applications
$Cu_{1.1}(In_{0.45}Al_{0.55})Se_2$ (Slightly Cu-rich) (0.8μm)	2.4	2	Co-existance of smaller and larger grains with densely packed structure	Isotropic [18]	Solar cells [35]
$Cu_{0.92}(In_{0.52}Al_{0.48})Se_2$ (Slightly Cu-poor) (0.75μm)	1.8	5	Rose-like morphology	Anisotropic [18]	High efficiency solar cells [36]
$Cu_1(In_{0.6}Al_{0.4})Se_2$ (Slightly In-rich/Al-poor) (0.45μm)	1.6	1	Platelet like structure	Twin-plane re-entrant edge growth [22]	High efficiency solar cells [37]
$Cu_1(In_{0.4}Al_{0.6})Se_2$ (Slightly In-poor/Al-rich) (0.6μm)	2.5	1.5 – 2	Morphology consisting of small and large spherical grains	Near Isotropic	High efficiency solar cells [36]
$CuIn_{0.5}Al_{0.5}Se_2$ (Stoichiometric films) (0.5 – 0.71μm)	2	1 – 2.5	Morphology with cubical shaped grains	Complete formation of CIAS without unreacted In or Se	High efficiency solar cells [37]

Table 5. Optical parameters of CBD CIAS thin films.

	Thickness (nm)	Band gap E_g (eV)	Absorption coefficient (α) 10^6 m^{-1}	Extinction coefficient (k) (λ = 1000 Å)	Dielectric constant (ε)	Refractive index (n)	Sellmeier parameters n_α	λ_0 (Å)
Near-stoichiometric	450	1.42	1.95	0.155	16.45	4.06	2.52	8671
	600	1.32	1.66	0.132	12.37	3.52	2.27	7971
	750	1.30	1.28	0.100	3.91	1.98	2.00	7156
	800	1.27	0.77	0.060	3.06	1.75	1.42	7121
Stoichiometric	500	1.44	12.2	0.97	9.75	3.27	1.7	9173
	625	1.35	9.78	0.77	9.52	3.18	1.7	9068
	710	1.24	8.60	0.68	8.77	2.69	1.7	8817

dex (n) and dielectric constant of CBD CIAS thin films were estimated using the expressions reported earlier [24, 41, 42] and are presented in Table 5. It was found that optical parameters of both near stoichiometric and stoichiometric CBD CIAS thin films decrease with film thickness which can be attributed to the improvement in crystallinity and decreased strain in the thicker films [24, 43, 44]. The spectral dependence of refractive index and the extinction coefficient of CBD CIAS thin films are presented in Figs. 6 and 7, respectively. The refractive index decreases with wavelength and film thickness in both near stoichiometric and stoichiometric CBD CIAS thin films [45] (Table 5). The decrease in refractive index with film thickness can be attributed to the strong effect of surface and volume imperfections on the macroscopic scale [46–49]. The decrease in refractive index with wavelength shows normal dispersion behavior of the material [45]. The decrease in extinction coefficient with wavelength [43, 44, 50] (Fig. 7) shows that the fraction of light lost due to scattering and absorbance decreases with wavelength.

The estimated refractive index values of CIAS thin films have been used to compute the Sellmeier parameters n_α and λ_0 [24]. The parameter λ_0 is an

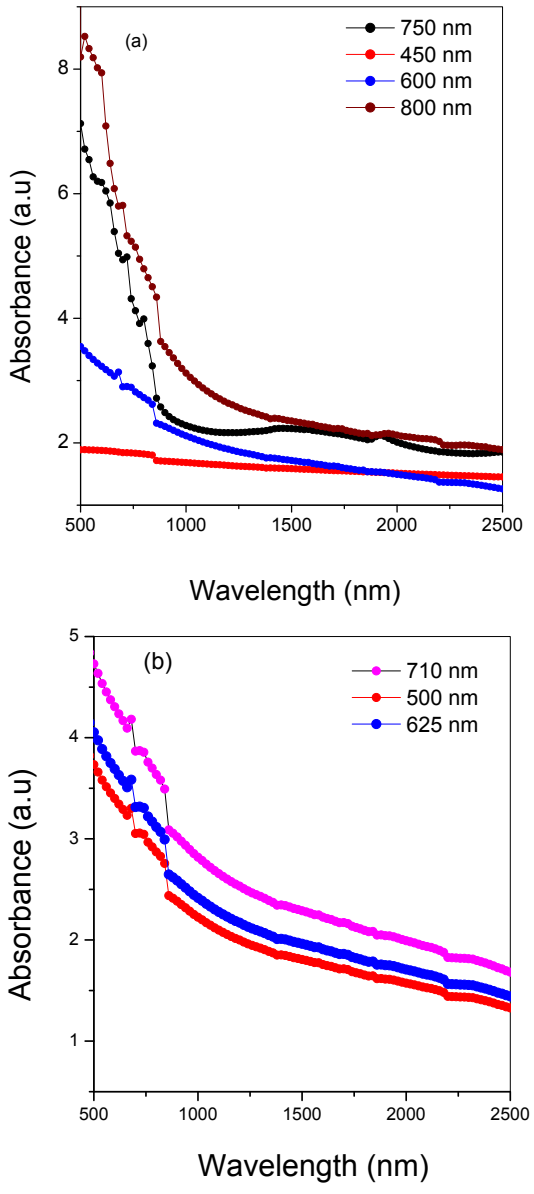

Fig. 4. Absorbance spectra of (a) near-stoichiometric and (b) stoichiometric CBD CIAS thin films.

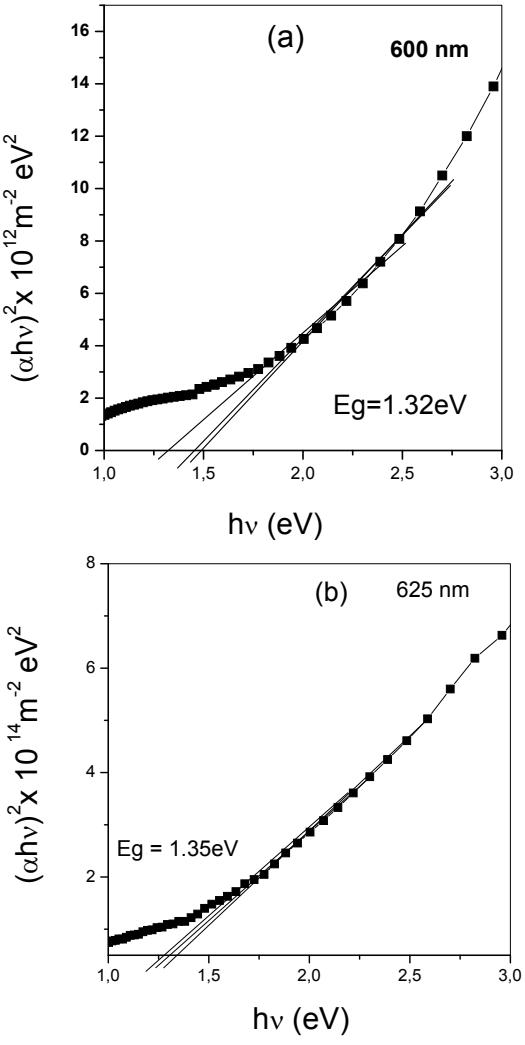

Fig. 5. Plot of $(\alpha h\nu)^2$ vs. $(h\nu)$ of (a) near-stoichiometric and (b) stoichiometric CBD CIAS thin films.

empirical one and its decreasing nature proves the real behavior of the semiconductor as reported earlier [24, 41]. The parameter n_α represents the refractive index for longer wavelength far from the absorption edge and this parameter is very useful to study the influence of the composition and growth conditions of the films on n_α. The observed value of n_α varies for the films of various composition (Tables 3 and 5) and this variation indicates that the deposited near stoichiometric CIAS films are of different composition. It is interesting to note that stoichiometric CIAS thin films have constant Sellmeier parameter n_α. Therefore Sellmeier parameter can also be used as a tool to find the stoichiometric/near-stoichiometric nature of CBD CIAS thin films.

4. Conclusion

Structural, compositional, morphological and optical properties of CBD CIAS films depend on the film composition and thicknesses. The growth

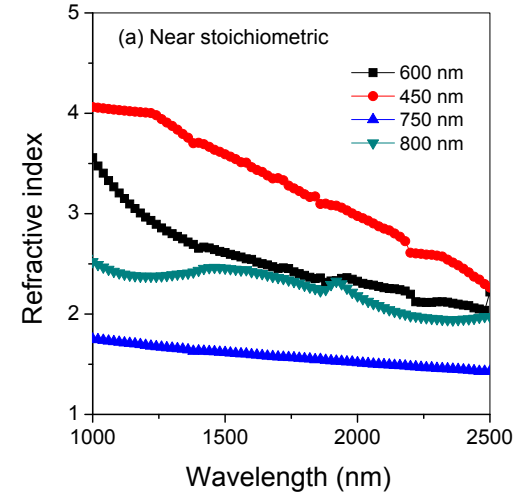

Fig. 6. Spectral distribution of refractive index of (a) near stoichiometric and (b) stoichiometric CBD CIAS thin films.

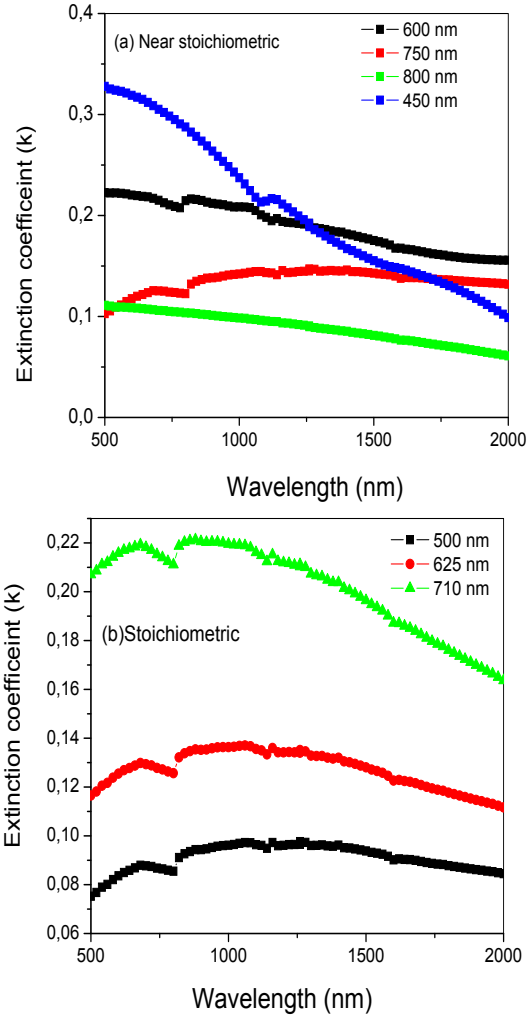

Fig. 7. Spectral distribution of extinction coefficient of (a) near-stoichiometric and (b) stoichiometric CBD CIAS thin films.

mechanism of CBD CIAS thin films has been identified from morphological analysis and reported in this paper. From the optical properties it has been found that the band gap of both near-stoichiometric and stoichiometric CBD CIAS films is suitable for photovoltaic applications.

Acknowledgements

The authors are grateful to the Secretary, Principal and Head of the Department of Physics, Kongunadu Arts and Science College, Coimbatore for their excellent encouragement and support. One of the authors (B.K) is grateful to express her thanks to Jawaharlal Nehru Memorial Fund for financial support.

References

[1] Bülent Başol M., Vijay Kapur K., Arvind Halani, Craig Leidholm, *Solar Energy Materials and Solar Cells*, 29 (1993), 163.

[2] Jackson P. et al., *Progress in Prog. Photovolt. Res. Appl*, 15 (2007), 507.

[3] Shafarman W.N., Klenk R., McCandless B.E., *Journal of Applied Physics*, 79 (1996), 7324.

[4] Rau U., Schmidt M., Jasenek A., Hanna G., Schock H.W., *Solar Energy Materials and Solar Cells*, 67 (2001), 137.

[5] Hayashi T. et al., *Solar Energy Materials and Solar Cells*, 93 (2009), 922.

[6] Paulson P.D., Haimbodi M.W., Marsillac S., Birkmire R.W., Shafarman W.N., *Journal of Applied Physics*, 91 (2002), 10153.

[7] MARSILLAC S., PAULSON P.D., HAIMBODI M.W., BIRKMIRE R.W., SHAFARMAN W.N., *Applied Physics Letters*, 81(2002), 1350.
[8] BHARATH KUMAR REDDY Y., SUNDARA RAJA V., *Semicond. Sci. Technol.*, 19 (2004), 1015.
[9] BHARATH KUMAR REDDY Y., SUNDARA RAJA V., *Solar Energy Mater. Solar Cells*, 90 (2006), 1656.
[10] BHARATH KUMAR REDDY Y., SUNDARA RAJA V., *Physica B*, 381 (2006), 76.
[11] ITOH E., SAITOH O., KITA M., NAGAMORI H., OIKE H., *Solar Energy Mater. Solar Cells*, 50 (1998), 119.
[12] DHANANJAY, NAGARAJU J., KRUPANIDHI S.B., *Solid State Communications*, 127 (2003), 243.
[13] HALGAND E., BERNEDE J.C., MARSILLAC S., KESSLER J., *Thin Solid Films*, 480 – 481 (2005), 443.
[14] DHANAM M., MANOJ P.K., PRABHU R.R., *J. Cryst. Growth*, 280 (2005), 425.
[15] KAVITHA B., DHANAM M., *Journal of Ceramic Processing Research*, 10 (2009), 652.
[16] REPINS I. et al., *Prog. Photovolta. Res. Appl*, 16 (2008), 235.
[17] SHI Y., JIN Z., LI C., AN H., QIU J., *Applied Surface Science*, 252 (2006), 3737.
[18] MERDES S. et al., *Thin Solid Films*, 516 (2008), 7335.
[19] KRUNKS M., MIKLI V., BIJAKINA O., MELLIKOV E., *Applied Surface Science*, 142 (1999), 356.
[20] KRUNKS M. et al., *Thin Solid Films*, 361 – 362 (2000), 61.
[21] CABALLERO R., GUILLEN C., *Applied Surface Science*, 238 (2004), 180.
[22] ZOPPI G., FORBES I., NASIKKAR P., MILES R.W., *Materials Research Society Symposium*, 1012 (2007), Y12.
[23] YANG L.C., CHENG C.Y., FANG J.S., *Journal of Physics and Chemistry of Solids*, 69 (2008), 435.
[24] DHANAM M., BALASUNDARPRABHU R., JAYAKUMAR S., GOPALAKRISHNAN P., KANNAN M.D., *Physica Status Solidi (a)*, 19 (1) (2002), 149.
[25] SCHEER R., DIESNER K., LEWERENZ H-J., *Thin Solid Films*, 268 (1995), 130.
[26] ZOUAOUI A., LACHAB M., HIDALGO M. L., CHAFFA A., LLINAREÁS C., KESRI N., *Thin Solid Films*, 339 (1999), 10.
[27] ARTAUD M.C., OUCHEN F., MARTIN L., DUCHEMIN S., *Thin Solid Films*, 324 (1998), 115.
[28] SHIRAKATA S., MURAKAMI T., KARIYA T., ISOMURA S., *Japanese Journal of Applied Physics*, 35 (1996), 191.
[29] KRUNKS M., BIJAKINA O., VAREMA T., MIKLI V., MELLIKOV E., *Thin Solid Films*, 338 (1999), 125.
[30] ORTEGA-LOPEZ M., MORALES-ACAVEDO A., *Thin Solid Films*, 330 (1998), 96.
[31] BIHRI H., MESSAOUDI C., SAYAH D., BOYER A., MZERD A., ABD-LEFDIL A., *Physica Stat. Solidi (A)*, 129 (1992), 193.
[32] OLEJNÍČEK J. et al., *Thin Soild Films*, 519 (2011), 5329.
[33] KADAM A.A., DHERE N.G., *Solar Energy Materials & Solar Cells*, 94 (2010), 738.
[34] HAYASHI T. et al., *Solar Energy Materials & Solar Cells*, 93 (2009), 922.
[35] SHAUKAT S.F., FAROQ R., KHAN M.A.U., RASHID A., DONG Y., *Information Technology Journal*, 6 (7) (2007), 1100.
[36] HO HAN S., HASOON F. S., PANKOW J.W., HERMANN A.M., D. H. LEVI, *Mater. Res. Soc. Symp. Proc.* Vol. 865 (2005) *Materials Research Society*, F1.3.1.
[37] NISHITANI M., NEGAMI T., TERACHI M., HIRAO T., *Japanese Journal of Applied Physics*, 31 (1992), 192.
[38] LÓPEZ-GARCÍA J., GUILLÉN C., *Thin Solid Films*, 517 (2009), 2240.
[39] SRINIVAS K., KUMAR J. N., CHANDRA G. H., UTHANNA S., *J Materials Science: Materials Electronics*, 17 (2006), 1035.
[40] BINDU K., SUDHA KARTHA C., VIJAYAKUMAR K.P., ABE T., KASHIWABA Y., *Solar Energy Materials and Solar Cells*, 79 (2003), 67.
[41] SHARMA R.P., SHARMA K.C., GARG J.C., *Journal of Physics D*, 24 (1991), 2084.
[42] SWANEPOEL R., *Journal of Physics E: Scientific Instruments*, 16 (1983), 1214.
[43] AGILAN S., MANGALARAJ D., NARAYANDASS S.K., VELUMANI S., IGNATIEV A., *Vacuum*, 81 (2007), 813.
[44] AGILAN S., MANGALARAJ D., NARAYANDASS S.K., MOHAN RAO G., *Physica B*, 365 (2005), 101.
[45] SHAH N.M. et al., *Thin Solid Films*, 517 (2009), 3639.
[46] MANIFACIER J.C., GASIOT J., FILLARD J.P., *Journal of Physics E*, 9 (1976), 1002.
[47] EHSHAN KH., TOMLIN S.G., *Journal of Physics D*, 8 (1975), 581.
[48] BEAGLEHOLE D., HUNDEERI O., *Physics Review B*, 2 (1970), 309.
[49] BENNET M.E., PORTENS J.O., *Journal of the Optical Society of America*, 51 (1969), 123.
[50] CHATTOPADHYAY K. K., SANYAL I., CHAUDHURI S., PAL A K., *Vacuum*, 42 (1991), 915.

Received 2012-12-25
Accepted 2013-07-27